Simulation study of the G=4 PAMAM dendrimer in water at different pH conditions

Juan J. Freire / *Pavlos* Efthymiopoulos / *Amirhossein* Ahmadi

Abstract

We report an analysis of Molecular Dynamics simulations carried out for the PAMAM-EDA dendrimer in water, considering neutral dendrimer, or high pH conditions, or assuming that all the amine groups are fully protonated at low pH (the addition of chloride counterions ensures the global charge neutrality of the system in this case). These simulations were performed considering the PCFF force-field with explicit consideration of hydrogen bonds and using the TIP3P molecular parameters for the water molecules. Our data indicate a remarkably different orientational distribution of dendrimer units for the two systems, low or high pH, with stronger segregation of dendrons in the former case Neutral dendrimers adsorb more water molecules.

Keywords

dendrimers · simulations · molecular dynamics · swelling · drug delivery systems

Juan J. Freire

Departamento de Ciencias y Técnicas Fisicoquímicas, Facultad de Ciencias,
Universidad Nacional de Educación a Distancia (UNED),

Paseo Senda del Rey 9, 28040 Madrid, Spain
e-mail: jfreire@invi.uned.es

Pavlos Efthymiopoulos
Amirhossein Ahmadi

Departamento de Ciencias y Técnicas Fisicoquímicas, Facultad de Ciencias,
Universidad Nacional de Educación a Distancia (UNED),
Paseo Senda del Rey 9, 28040 Madrid, Spain

1 Introduction

The polyamidoamine dendrimers with an ethylenediamine core (PAMAM-DEA) are now commercially available and have a great potential in different applied fields [1]. In these particular dendrimers, both primary and tertiary (or peripheral and inner) amino groups can be protonated and this protonation is strongly influenced by the physiological conditions of the medium, particularly the solution pH. (All amine groups are expected to be fully protonated at low pH and they should be neutral in high pH solution). Due to their structural flexibility, size and shape of the dendrimers can be altered by the absence or presence of strong repulsive interaction between groups with positive charges, allowing or not for the inclusion of other molecules. This feature suggests a promising way to module the transportation and delivery of drugs.

Molecular Dynamics (MD) simulations can be a useful tool to predict properties of complex molecular systems [2]. Atomistic interactions can be described through the potential energy terms contained in different force-field files. The simulations have the advantage of predicting some properties that are not accessible from experiments in an easy way, as the detailed structure in the interior of a dendrimer molecule, including free-space and distribution of solvent molecules and counter-ions. The particular case of the PAMAM-EDA molecule including four generations (G4) has been extensively studied considering different degrees of protonation [3]. The earlier simulations [4] for this system yielded very different sizes depending on the protonation level. However, these results are in contradiction with the most recent and reliable experimental estimations obtained from small angle neutron scattering (SANS) measurements [5] which show a weak variation of the dendrimer size with pH. This lack of significant influence of the solution pH on dendrimer size was also previously observed in experiments dendrimers of higher generation number [6]. More recently, new simulation results have achieved a better agreement with the experimental data for the G=4 case [7]. These new results are based in a modification of the general purpose, or universal, *Dreiding* force-field [8] that explicitly considers some types of hydrogen bonds.

In a similar way, we have investigated the role of hydrogen bonds in the alternative more specific, class II, *PCFF* force-field [9], using also the TIP3P molecular parameters and partial charges for water [10]. With these specifications we have been able to find a similarly good reproduction of the neutron scattering data for G=4 PAMAM-EDA dendrimers with different degrees of protonation [11]. In the present work, we explored some features revealed from the analysis of the initial 2ns of the simulation trajectories, in particular the location of the amine groups within the dendrimer, the angular distribution of the density around the dendrimer center for conformations of neutral and charged dendrimers and the time evolution of the mean number of water molecules associated to amines located at different shells.

2 Models and methods

We performed our molecular dynamics simulations using the *Materials Studio* (MS) [12] software suite and the open source MD software DL-POLY [13]. We easily constructed the initial dendrimer configurations in vacuum using the MS module "*Visualizer*" building tools. These configurations were subsequently minimized. The minimizations were carried out with the "*Discover*" module also included in the MS suite.

We verified that the neutral molecules cannot have access to part of the representative open conformations if we directly use initial conformations provided by the MS building tools. (However, we did not observe a similar problem for the protonated molecules). We performed some minimizations of the protonated dendrimer structure in vacuum with an adequate cut-off of the Van der Waals interactions and a high dielectric constant. These specifications do not try to provide a realistic description of the isolated dendrimer molecule in vacuum, but they are needed to ensure a sufficiently open starting conformation. The resulting open protonated structures were then reconverted as neutral dendrimers. In all cases, the atom partial charges within the dendrimer molecule were set according to the charge equilibration method [14] based on the equilibration of atomic electrostatic potentials with respect to a local charge distribution.

Employing the MS module "*Amorphous Cell*", we constructed relaxed simulation boxes with periodic boundary conditions of size *L*. In these boxes we included a dendrimer molecule together with 4,000 water molecules. In the case of the protonated dendrimers, we also add 126 chlorine anions that neutralize all the charged (tertiary and primary) amine groups.

Preliminary simulations were performed at constant pressure, *P*=1 atm. and temperature, *T*=300 K, (in the NPT ensemble) until we reach a constant value of the density. Final MD simulations were performed at constant temperature (NVT ensemble) using the open source molecular dynamics software *DL-POLY* [14]. This software offers a high flexibility when it comes to incorporating new force-field parameters [15]. Dielectric constant was fixed to the vacuum value, ε=1.

Our final trajectories are extended over 10^6 simulations steps of 1 fs. We have verified that total energy and temperature oscillate around stabilized mean values in the analysed trajectories.

In previous simulations for PAMAM-EDA [7] with the *Dreiding* force-field, experimental dendrimer sizes could only be reproduced through an explicit description of hydrogen bonds. We have verified that the direct use of the *PCFF* force-field for the dendrimer atom interactions also gives a substantial variation of the dendrimer size with pH, similar to that found with the first version of *Dreiding* [2]. Therefore, this variation is inconsistent with the experimental data. Consequently, we also have incorporated hydrogen bonds to the original *PCFF* force-field. We have investigated a simple modification based in the functional form and parameters considered in the hydrogen bond terms proposed for *Dreiding* [7]. These terms depend on the distance between donor and acceptor atoms and also on the angle formed by their respective bonds with the H atom. The experimental data are closely reproduced when the different values for the potential well parameter are reduced to be one third of the values employed with the *Dreiding* force-field. These values were reported in Table S3 of the Supporting Information for Ref. [7]. We have not introduced any additional change in the PCFF parameters for the dendrimer molecules and their interaction with water.

3 Results and discussion

Once we have achieved an adequate reproduction of the molecular sizes through the consideration of explicit hydrogen bond interactions, we have analyzed different conformational properties corresponding to these simulations that may help us to describe the space distribution of atoms. As a reference for the location of the different dendrimer shells, we show in Tab. 1 the mean location of the different amine groups (the 2 amine groups in the molecule center are omitted).

It can be observed that the outer amine groups belonging to the protonated molecules are at a significantly higher distance with respect to the neutral molecule than the inner groups. The overall mean distance is also greater for the protonated molecules. However, the mean radius of gyration of the neutral and protonated molecules obtained from the same simulation trajectories are more similar, 20.2 and 21.7 Å, respectively [11]. These results are satisfactorily close to the values 21.1 and 22.1 obtained for the same dendrimers with the modified *Dreiding* force-field [7] and with the 21.4 value obtained from SANS [5] (without significant pH variation). We have not found significant differences in the mean density profiles between the two types of molecules. This suggests that the main difference between both molecules is not in the size or the radial distribution (obtained as an orientational and conformational average) but in the orientational density distribution corresponding to the different conformations. We have analysed this property in the present work.

Juan J. Freire / Pavlos Efthymiopoulos / Amirhossein Ahmadi

Tab. 1. Mean distance of the amine N atoms corresponding to different amine shells from the dendrimer center (in Å).

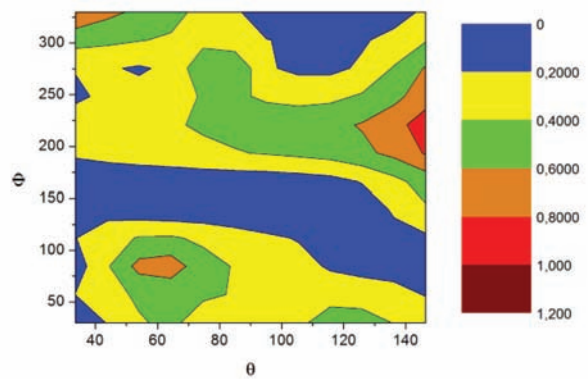| Shell	Number of amines	Neutral	Protonated
1	4	9.1	9.4
2	8	14.8	14.5
3	16	18.6	18.7
4	32	21.2	22.2
5	64	22.2	25.0
Overall mean distance		21.5	23.5
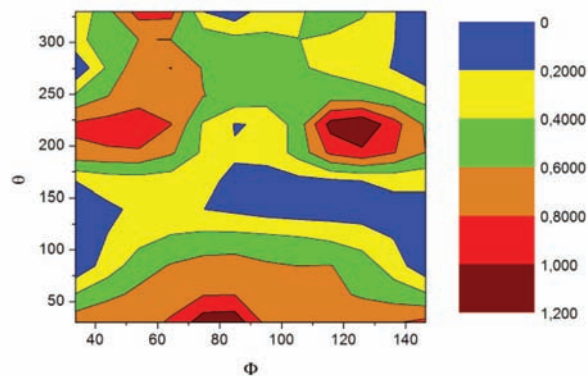
Fig. 2. Contour curves of the dendrimer density (in g./cm^3) obtained for the neutral dendrimer at R=11.25 Å
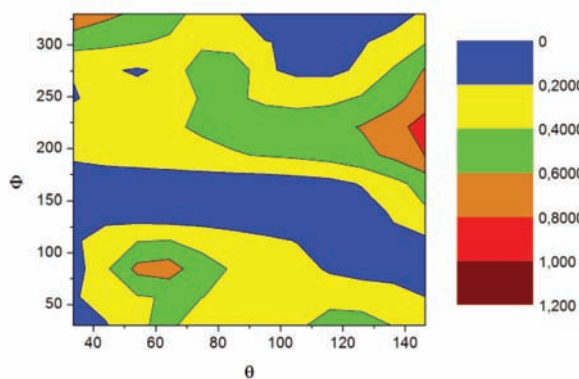
Fig. 1. Contour curves of the dendrimer density (in g./cm^3) obtained for the protonated dendrimer at *R*=11.25 Å
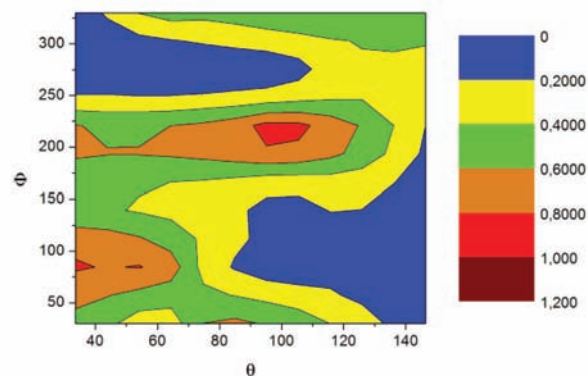

Fig. 3. Contour plot of the dendrimer density (in g./cm^3) obtained for the protonated dendrimer at *R*=15.75 Å

We report the angular distribution of the dendrimer density distribution corresponding to the last step of our equilibrated trajectories. Using an arbitrarily defined set of polar coordinates with origin at the dendrimer center, we create a three-dimensional mesh of elements defined by equally spaced interval of R, cos(θ) and ϕ and evaluate the normalized density (in macroscopic units) of dendrimer atoms in each one of these elements. In Figs. 1 to 4, we show contour plots of the density corresponding to two different values of R, R=11.25 and 15.75 Å, closer to the dendrimer core and at an intermediate shell, see Tab. 1.

It can be observed that the conformations of neutral and protonated dendrimer show significantly different orientational atomic distributions. The neutral dendrimer shows a more continuous distribution, while the protonated molecule shows a significant gap that divides the molecule into separated regions. This segregation is possibly associated to the division into different dendrons.

The snapshots of these different distributions provided in Fig. 2 of Ref. [7] (previous simulations with the *Dreiding* potential) are in agreement with this description. However, the discussion was not focused in a dendron segregation effect but in a transition from dense core to dense shell conformations

Fig. 4. Contour curves of the dendrimer density (in g./cm^3) obtained for the neutral dendrimer at *R*=15.75 Å.

characterized by the different peaks in the radial density profiles. These two forms are reminiscent of the older Boris-Rubinstein [16] and de Gennes-Hervet [17] theoretical models. Snapshot of our protonated and neutral dendrimers can also be observed in Fig. 5 and they are also in agreement with some degree of dendron segregation for the protonated molecules. As we have described above, our simulations do not show important
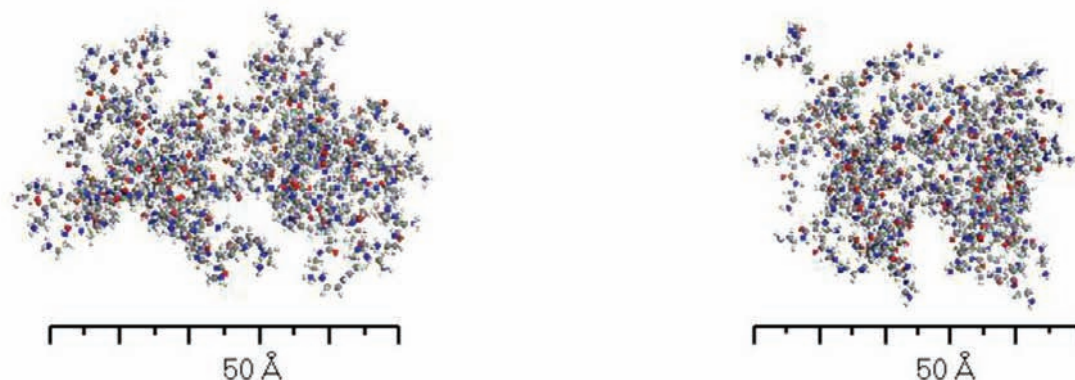
Fig. 5. Snapshots of the protonated (left) and neutral (right) dendrimers.

differences in the dendrimer radial density profiles [11] but they point out a more significant change in the angular distribution.

The different dendrimer distributions lead to different forms of solvent penetration [11]. In the neutral dendrimer, a more uniform distribution implies a greater overall permeability over a similar molecule volume. This way, more water molecules can be "adsorbed" i.e., they can be located closer to the tertiary amine groups. However, in the case of the protonated dendrimer, some water molecules can be located closer to the dendrimer center, penetrating through the gaps between dendrons, although not so many molecules can be located close to the ternary amines in the intermediate shells.

This description is consistent with Fig. 6 showing the time evolution of the number of water molecules closer to the amine groups in the core, intermediate and external shells. It can be observed that the water molecules are able to move inside the dendrimer and their location alternates between the shells. More water molecules can penetrate to the core in the protonated dendrimer, but the total number of water molecules in the intermediate shells is higher for the neutral molecule. Consequently, the neutral molecule adsorbs more water molecules and the total number of external water molecules i.e. closer to the outer shell) is greater for the protonated case.

Experimental SANS data cannot describe these differences since the only provide an estimation of the dendrimer global size. NMR spectroscopy, however, gives more information at local scale. A recent NMR study for functionalized G4 PAMAM dendrimers [18] indicates that a higher number of water molecules interact with the dendrimer molecule in high pH conditions. This is in qualitative agreement with the significantly greater number of water molecules associated to the dendrimer intermediate shells shown in Fig. 6.

4 Conclusions

We have performed Molecular Dynamics simulations of low and high pH aqueous solutions of G=4 PAMAM-EDA dendrimers using a modified PCFF force-field, where the hydrogen bonds are taken explicitly into account. The size of the
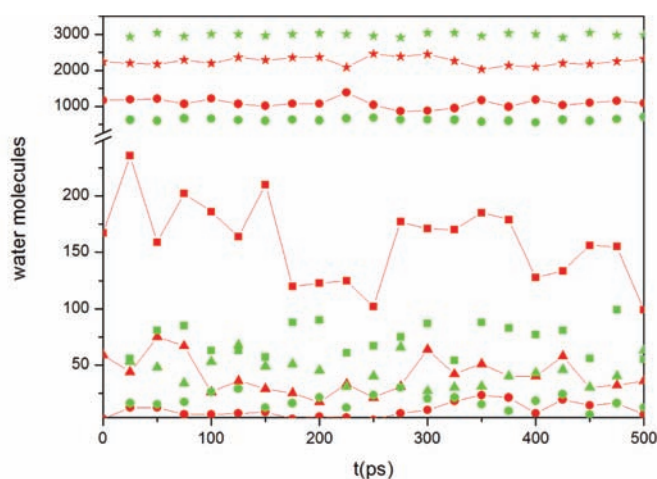

Fig. 6. Evolution with time of the number of water molecules closer to the amine groups in different dendrimer shells. Symbols (green) correspond to the protonated molecules. Symbols and lines (red) correspond to the neutral molecules. From top to bottom, stars: fifth shell (outer); diamonds: forth shell; squares: fourth shell; triangles: second shell; circles: first shell (core).

protonated dendrimer was found to be slightly larger than the neutral one, though both values are close to the experimental SANS data [11]. However, the internal configurations of the two dendrimers are significantly different. A detailed analysis of the spatial dendrimer atom distribution reveals a more noticeable orientational segregation for the protonated molecule, low pH. Also for this case, the location of a lower number of water molecules in the intermediate dendrimer shell together with a greater permeation of water molecules to the core for suggest a significant degree of dendron segregation.

It should be noted that the apparent pH driven transition from a more permeable, more uniform, dendrimer distribution at high pH (neutral dendrimer) to a dendron segregated form at low pH (protonated dendrimer) may have implications in order to understand the performance of PAMAM-EDA molecules in the transport or delivery of different drugs or other types of pH modulated biological applications, even though this dendrimer does not show a noticeable change of size at varying pH values.

Juan J. Freire / Pavlos Efthymiopoulos / Amirhossein Ahmadi

References

1 Fréchet J. M. J., Tomalia D. A., *Dendrimers and Other Dendritic Polymers*. Wiley, Chichester, England (2001). DOI: 10.1002/0470845821

2 Frenkel D., Smit B., *Understanding Molecular Simulation: From Algorithms to Applications*. Academic Press, San Diego, California (1996).

3 Freire J. J., *Realistic numerical simulations of dendrimer molecules*. Soft Matter, 4(11), 2139-2143 (2008). DOI: 10.1039/B804687E

4 Maiti P. K., Çağin T., Lin S-T., Goddard III W. A., *Effect of solvent and ph on the structure of PAMAM dendrimers*. Macromolecules, 38(3), 979-991 (2005). DOI: 10.1021/ma049168l

5 Chen W-R., Porcar L., Liu Y., Butler P. D., Magid L. J., *Small angle neutron scattering studies of the counterion effects on the molecular conformation and structure of charged G4 PAMAM dendrimers in aqueous solutions*. Macromolecules, 40(16), 5887-5898 (2007). DOI: 10.1021/ma0626564

6 Nisato G., Ivkov R., Amis E. J., *Size invariance of polyelectrolyte dendrimers*. Macromolecules, 33(11), 4172-4176 (2000). DOI: 10.1021/ma991474p

7 Liu Y., Bryantsev V. S., Diallo M. S., Goddard III W. A., *PAMAM Dendrimers Undergo ph Responsive Conformational Changes without Swelling*. Journal of the American Chemical Society, 131(8), 2798-2799 (2009). DOI: 10.1021/ja8100227

8 Mayo S. L., Olafson B. D., Goddard III W. A., *DREIDING: a generic force field for molecular simulations*. The Journal of Physical Chemistry, 94(26), 8897-8909 (1990). DOI: 10.1021/j100389a010

9 Sun H., Mumby S. J., Maple J. R., Hagler A. T., *An ab-initio cff93 all-atom force-field for polycarbonates*. Journal of the American Chemical Society, 116(7), 2978-2987 (1994). DOI: 10.1021/ja00086a030

10 Jorgensen W. L., Chandrasekhar J., Madura J. D., Impey R. W., Klein M. L., *Comparison of simple potential functions for simulating liquid water*. Journal of Chemical Physics, 79, 926 (1983). DOI: 10.1063/1.445869

11 Ahmadi A., McBride C., Freire J. J., *Molecular Dynamics simulations of the protonated G4 PAMAM dendrimer in an ionic liquid system*. The Journal of Physical Chemistry B, 117(48), 15157–15164 (2013). DOI: 10.1021/jp402586s

12 Accelrys Software Inc. San Diego, California

13 Smith,W., Yong C. W., Rodger P. M., *Dl_poly: application to molecular simulation*. Molecular Simulations, 28(5), 385-471 (2002). DOI: 10.1080/08927020290018769

14 Rappe A. K., Goddard III W. A., *Charge equilibration for molecular-dynamics simulations*. The Journal of Physical Chemistry, 95(8), 3358-3363 (1991). DOI: 10.1021/j100161a070

15 Ahmadi A., McBride C., Freire J. J., Kajetanowicz A., Czaban J., Grela C. J., *Force Field Parametrization and Molecular Dynamics Simulation of Flexible POSS-Linked (NHC; Phosphine) Ru Catalytic Complexes*. The Journal of Physical Chemistry A, 115(43), 12017-12024 (2011). DOI: 10.1021/jp2062332

16 Boris D., Rubinstein M., *A self-consistent mean field model of a starburst dendrimer: Dense core vs dense shell*. Macromolecules, 29(22), 7251-7260 (1996). DOI: 10.1021/ma960397k

17 de Gennes P. G., Hervet H., *Statistics of starburst polymers*. Journal de Physique Lettres, 44(9), 351-360 (1983). DOI: 10.1051/jphyslet:01983004409035100

18 Bányai I., Kéri M., Nagy Z., Berka M., Balogh L. P., *Self-diffusion of water and poly(amidoamine) dendrimers in dilute aqueous*. Soft Matter, 9(5), 1645-1655 (2013). DOI: 10.1039/C2SM26726H